Artificial neural network detects human uncertainty

Alexander E. Hramov, Nikita S. Frolov, Vladimir A. Maksimenko, Vladimir V. Makarov, Alexey A. Koronovskii, Juan Garcia-Prieto, Luis Fernando Antón-Toro, Fernando Maestú, and Alexander N. Pisarchik

Citation: Chaos **28**, 033607 (2018); doi: 10.1063/1.5002892
View online: https://doi.org/10.1063/1.5002892
View Table of Contents: http://aip.scitation.org/toc/cha/28/3
Published by the American Institute of Physics

CHAOS 28, 033607 (2018)

Artificial neural network detects human uncertainty

Alexander E. Hramov,[1,2,a)] Nikita S. Frolov,[1] Vladimir A. Maksimenko,[1] Vladimir V. Makarov,[1] Alexey A. Koronovskii,[2] Juan Garcia-Prieto,[3,4] Luis Fernando Antón-Toro,[3] Fernando Maestú,[3] and Alexander N. Pisarchik[1,3,b)]

[1]*Artificial Intelligence Systems and Neurotechnologies, Yuri Gagarin State Technical University of Saratov, Politehnicheskaya, 77, Saratov 410054, Russia*
[2]*Saratov State University, Astrakhanskaya, 83, Saratov 410012, Russia*
[3]*Center for Biomedical Technology, Technical University of Madrid, Campus Montegancedo, 28223 Pozuelo de Alarcon, Madrid, Spain*
[4]*Department of Industrial Engineering, Laboratory of Electrical Engineering and Bioengineering, Universidad de La Laguna, Tenerife, Spain*

(Received 1 September 2017; accepted 18 February 2018; published online 5 March 2018)

Artificial neural networks (ANNs) are known to be a powerful tool for data analysis. They are used in social science, robotics, and neurophysiology for solving tasks of classification, forecasting, pattern recognition, etc. In neuroscience, ANNs allow the recognition of specific forms of brain activity from multichannel EEG or MEG data. This makes the ANN an efficient computational core for brain-machine systems. However, despite significant achievements of artificial intelligence in recognition and classification of well-reproducible patterns of neural activity, the use of ANNs for recognition and classification of patterns in neural networks still requires additional attention, especially in ambiguous situations. According to this, in this research, we demonstrate the efficiency of application of the ANN for classification of human MEG trials corresponding to the perception of bistable visual stimuli with different degrees of ambiguity. We show that along with classification of brain states associated with multistable image interpretations, in the case of significant ambiguity, the ANN can detect an uncertain state when the observer doubts about the image interpretation. With the obtained results, we describe the possible application of ANNs for detection of bistable brain activity associated with difficulties in the decision-making process. *Published by AIP Publishing.*
https://doi.org/10.1063/1.5002892

Nowadays, artificial neural networks (ANNs) are widely used in different areas of science, engineering, and technology. In neuroscience, ANNs are able to classify motor-related neural signals, pathological brain activity, and psychiatric disorders. Although the problem of classification of well-established brain states is already successfully solved with ANNs, the ability of this tool to classify bistable states, when uncertainties in the human brain result in the uncertainties of input neurophysiological data, is still poorly understood. In this research, we use the ANN approach to classify bistable brain states which occur during the perception of an ambiguous visual object. We demonstrate that the ANN can distinguish states of certainty and doubt in the human brain and define features of the decision making process.

I. INTRODUCTION

Artificial neural networks (ANNs) are a useful instrument for complex and multivariate data analysis. From a mathematical point of view, they represent a generalized model of information processing inspired by a mammal's neural system.[1] The ANN consists of a large number of interconnected elementary computational units (artificial neurons) which form a complex multi-layer network where information is transferred from layer to layer. Each layer of the network processes the input information embodying the concept of multi-level human perception. Thus, the aim of this simple mathematical model is to assimilate information in a similar way as the human brain. The recent progress in computational systems' performance caused a huge interest in the development of ANNs among the scientific community and, therefore, initiated intensive research on effective approaches to their architecture and widespread applications in different areas of science and technology (see Refs. 2–4 for review).

In the neuroscience area, ANNs are very promising for the analysis of human brain activity and especially for cognitive engineering.[5] Recent scientific papers report on the application of ANNs for the analysis of EEG[6] and MEG[7] signals, fMRI images,[8] and other clinical data.[9] One important ANN application is the detection and classification of brain states by analyzing neurophysiological data.[10,11] The classification of brain states is of great importance for the development of brain-computer interfaces (BCIs), where effective detection of neuronal activity is required.[12,13] In this context, ANNs are known to be able to classify motor-related neural signals,[14,15] detect pathological brain activity,[16,17] psychiatric disorders,[18,19] etc.

The ANN approach to the analysis of neurophysiological data can be described as follows. The ANN receives, as an input, a set of EEG or MEG signals and converts them to a binary output. The ANN being trained on some known data

[a)]Electronic mail: hramovae@gmail.com
[b)]Electronic mail: alexander.pisarchik@ctb.upm.es

set to learn features of the input data associated with a certain brain state, becomes able to extract similar states from a large amount of unknown input data. This is the advantage of the ANN in the detection of highly reproducible events in the human brain, e.g., motor-related activity, epileptic seizures, etc.

On the other hand, the application of ANNs in cases when the brain is not able to select any stable long-term state and exhibits multiple abrupt switches between different states is much more challenging. This situation is common in decision-making processes when a person lacks information and, as a consequence, doubts about the decision.[20] In this case, two interesting questions arise: (i) How does the ANN, being trained to identify brain states associated with firmly adopted decisions, find a state of uncertainty in decision-making? and (ii) How can the ANN be applied for detecting human uncertainty in decision-making via EEG and MEG signals? The answers to these questions are important for understanding fundamental aspects of the brain's cognitive activity and practical use of artificial intelligence and deep learning tools aimed at the development of BCIs for improving human performance in decision-making. Moreover, this ANN application for decision-making in uncertain conditions is very promising for intelligent robotics and information systems.

According to the above motivation, in this paper, we apply, for the first time to the best of our knowledge, ANNs for detection and recognition of human uncertainty in decision-making. For this purpose, we consider the human MEG trials corresponding to the perception of ambiguous visual stimuli. The perception of such stimuli is associated with a multistable decision-making process, since the same object can be interpreted in different ways. While the interpretation of most bistable objects is random, there are some bistable stimuli for which the degree of ambiguity can be easily controlled, and this allows the selection of one or another interpretation. One of these stimuli is the Necker cube.[21] This is a 2D cube projection with transparent faces and visible edges [see Fig. 1(a)]. The contrast of the three middle lines centered in the left middle corner is defined by the parameter $I \in [0, 1]$ used as a control parameter. Bistability in the cube perception consists in the interpretation of this 2D-object as a 3D-object which can be oriented in two different ways, left-oriented or right-oriented. One can see from Fig. 1(a) that the cubes with $I = 0.1$ and $I = 0.9$ can easily be interpreted as left-oriented and right-oriented, respectively. However, the Necker cubes with $I \simeq 0.5$ cannot be unambiguously interpreted, especially if the decision time is too short.

Our MEG experiments carried out with five volunteers demonstrated that the level of uncertainty in the Necker cube interpretation significantly increased for $I \simeq 0.5$ due to strong image ambiguity. Figure 1(b) shows the level of uncertainty, $\Psi(I)$, in interpretation of the bistable image, defined as

$$\Psi(I) = \begin{cases} 2P_R(I), & I < 0.5, \\ 2P_L(I), & I \geq 0.5, \end{cases}$$

where $P_R(I)$ and $P_L(I)$ are probabilities for the right-oriented and left-oriented cube perception, respectively. As expected,

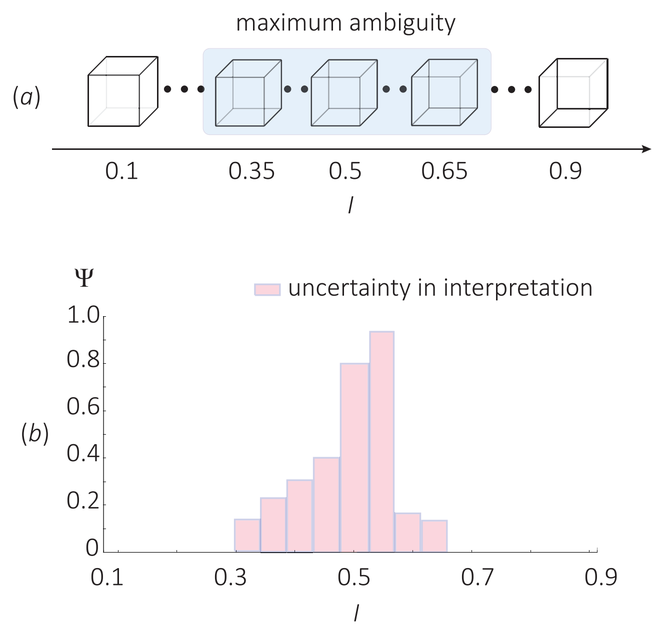

FIG. 1. (a) Ambiguous images of the Necker cube with different edges intensity I, presented to subjects during the experiments. The cubes with $I < 0.5$ and $I > 0.5$ are usually interpreted as left-oriented and right-oriented, respectively. (b) Typical level of uncertainty in the Necker cube interpretation by a subject.

a high degree of uncertainty ($\Psi(I) > 0.8$) is observed for $I \simeq 0.5$. We suppose that an ANN trained to identify brain states associated with left-oriented and right-oriented interpretations is able to describe the decision-making process and detect the degree of uncertainty. This would allow to detect doubts during the decision-making process.

The structure of the paper is as follows. In Sec. II, we describe the materials and methods used in our neurophysiological experiments on the MEG recording, subjects, and the procedure of mathematical processing using ANN algorithms and statistical analysis. The results on the MEG data processing and classification of the brain states using ANN are presented and discussed in Sec. III. Finally, the results are summarized in Sec. IV.

II. MATERIALS AND METHODS

A. Experimental setup

Neurophysiological data was acquired by using a 306-channel (102 magnetometers and 204 planar gradiometers) Vectorview MEG system (Elekta AB, Stockholm, Sweden) placed inside a magnetically shielded room (Vacuum Schmelze GmbH, Hanau, Germany) at the Laboratory of Cognitive and Computational Neuroscience of the Center for Biomedical Technology of the Technical University of Madrid (Spain). The head shape was obtained by using a three-dimensional Fastrak digitizer (Polhemus, Colchester, Vermont). Three fiducial points (nasion, left and right preauricular points) and at least 300 points on the scalp surface were acquired for each subject. In addition, four head position indication (HPI) coils were placed on the subject's scalp, two on the mastoids, and two on the forehead. The HPI coils position was also acquired using the Fastrak device, and continuous head position estimation was used during the recording in order to track head movements. A vertical electrooculogram of the left eye was used to capture blinks and eye movements. The MEG data were acquired using a sampling rate of 1000 Hz and an online anti-alias bandpass filter between 0.1 and 330 Hz.

B. Participants

Five healthy unpaid subjects, males and females, between 26 and 30 years old with normal or corrected-to-normal visual acuity participated in the experiments. All of them provided written informed consent before participating in the experiment. The experimental studies were performed in accordance with the Declaration of Helsinki at the Center for Biomedical Technology of the Technical University of Madrid.

C. Visual stimuli

The ambiguous image was the Necker cube[21] frequently used in experimental[22–25] and theoretical studies.[23,26,27] This image is seen as a cube with transparent faces and visible edges; an observer without any perception abnormalities perceives the Necker cube as a 3D-object due to the specific position of the cube's edges. Bistability in the cube perception consists in the interpretation of the Necker cube as being oriented in two different ways, i.e., left-oriented or right-oriented. The contrast of the three middle lines centered in the left middle corner, $I \in [0, 1]$, was used as a control parameter. The values $I = 1$ and $I = 0$ correspond, respectively, to 0 (white) and 255 (black) pixels' luminance of the middle lines. Therefore, the contrast parameter in the 8-bit grayscale palette was defined as $I = y/255$, where y is the brightness level of the middle lines. Visual stimuli were presented with the help of Cogent (a graphics toolbox for MATLAB) and the contrast parameter of the presented stimuli was controlled by a software specially developed for this study.

D. Experimental design

Each subject took part in two experimental sessions. The structure of both sessions was the same except for one feature: in the first session, the subject was instructed to press either a left or right key depending on his/her interpretation of the Necker cube in each demonstration, while in the second session, the button pressing was excluded. The data obtained in the first session were analyzed after the key press to estimate the participant's uncertainty level based on the experimental results [a typical level of uncertainty can be seen in Fig. 1(b)]. The aim of the second session was to collect the MEG data for a further analysis using ANN trained on the data of the first session. The MEG data recorded in the second experimental session were not associated with the motor-related brain activity and therefore suitable for the analysis of the cognitive activity involved in the decision-making process.

The structure of each session was as follows. (i) First, background MEG activity was recorded for 2 min, while the subject was sitting comfortably with open eyes. (ii) Then, a set of Necker cubes with different wireframe contrasts were presented during approximately 20 min. (iii) Finally, another 2-min background MEG was recorded while the subject was sitting comfortably with closed eyes. As a result, the whole session took about 25 min.

In this experiment, we used 15 Necker cubes with randomly chosen contrast parameters from the set $I = (0.1, 0.15, 0.3, 0.4, 0.47, 0.48, 0.49, 0.5, 0.51, 0.52, 0.53, 0.6, 0.7, 0.85, 0.9)$. Each contrast was presented 15 times. Each image was presented to the participants for a short period of time, randomly chosen between 0.8 s and 1.2 s. It is known from the literature that the mean duration of a visual percept can vary from one second to several minutes depending on individual features of the observer and stimulus conditions,[28] while the mean response times are rather consistent and vary only by a few hundred milliseconds.[29] The most common experimental length for each perception of the Necker cube was found to be approximately 1 s.[30] Therefore, in order to fix the first impression of the person and avoid switches between two possible percepts, the image exhibition in our experiments was limited to $\nu \in [0.8, 1.2]$ s.

The short duration of stimulus presentation is also needed to reduce the stabilization effect.[31] Indeed, the probability of the configuration persisting until the subsequent presentation is known to be highly dependent on how long it was seen before the stimulus was removed.[31] Only when the perceptual configuration was consistently seen for a relatively long time before the stimulus disappeared, there was a high probability of it persisting to the next stimulus presentation. Since the required time for consistent observation of the Necker cube is about 1 s,[31] the stimulus exhibition for a shorter time diminished the "memory" effect. The random sequence of the Necker cubes with different values of the control parameter I also prevented the appearance of the perception stabilization. Finally, to draw away the observer's attention and make the perception of the next Necker cube independent of the previous one, different abstract pictures were randomly exhibited for about $\eta \in [4.20, 5.25]$ s between demonstrations of the different Necker cube images.

E. MEG signals pre-processing

Figure 2(a) shows the block diagram illustrating the main steps for the MEG data analysis. First of all, we collected an entire MEG dataset obtained during the described experiment. Afterwards, the MEG signals were pre-processed via filtration and artifact removal techniques. Finally, the pre-processed MEG recordings were normalized and fed to trained ANN. In further subsections, we provide a detailed description of the above-mentioned data analysis steps.

After a successful completion of the experiment, MEG signals recorded by magnetometers (102 sensors) were prepared for subsequent analysis and classification via ANN. To extract the magnetic field activity generated by the brain and remove undesired components from the entire MEG signals, we applied band-pass filtration in the frequency range from 5 to 30 Hz. Thus, we removed low-frequency artifacts (< 5 Hz) and high-frequency oscillations (> 30 Hz), not related to cognitive brain activity. Also, undesired MEG artifacts associated with breathing, heartbeat, eye movement, and blinking

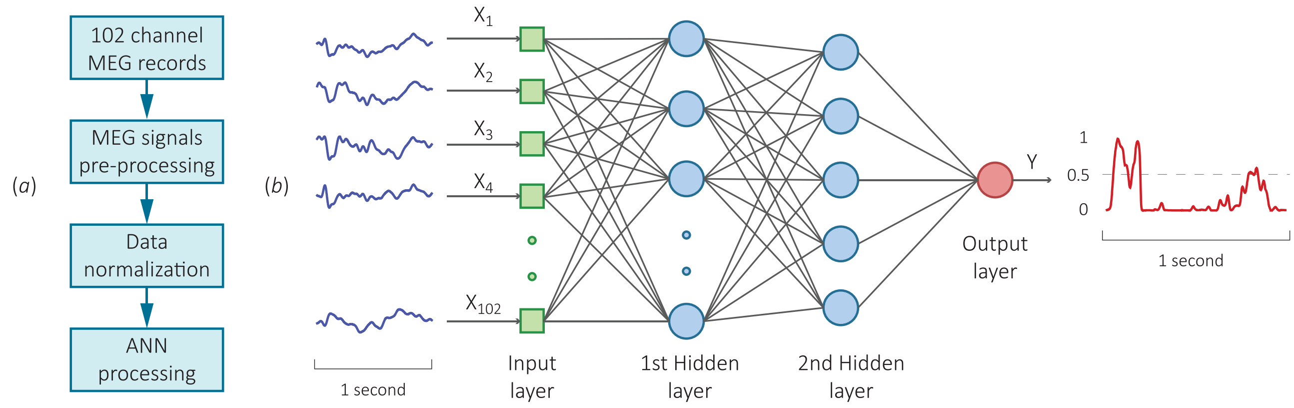

FIG. 2. (a) Block diagram illustrating main procedures carried out to prepare multivariate MEG signals for ANN processing. (b) Structure of the feed-forward multilayer perceptron (MLP) neural network. One can see typical input MEG trials X_n (*blue curves*), corresponding to brain activity after demonstration of left-oriented Necker cube and typical MLP response Y (*red curve*). The subscripts of X_n indicate the MEG channel number ($n = 1,\ldots,102$).

were removed using the temporal signal-space separation (tSSS) method by Taulu and Hari.[32] Finally, the MEG signals were normalized and scaled to the [–1, 1] range for each channel separately.

F. Artificial neural network

ANN is a data-processing tool which operating principle is adopted from human brain mechanisms of information processing. Like the human brain, the ANN consists of a large number of interconnected neurons, which play a role of elementary computing units. The simplest and most widely used ANN architecture is a multilayer perceptron (MLP). MLP represents a feed-forward neural network, where information signal $\mathbf{X}$ is fed to an input layer of the network and sequentially travels towards an output layer, which generates output signal Y. MLP was successfully applied for classification and pattern recognition in neuroscience and biomedical applications.[6–8,33] In our study, we use MLP for classification of different human brain states emerging during the perception of ambiguous images. MLP was implemented through the Neural Network Toolbox of MATLAB. Here, we describe an instantaneous human brain state as an N-dimensional column vector

$$\mathbf{X}^j = (x_1(t_j), x_2(t_j), \ldots, x_N(t_j))^T, \tag{1}$$

an instantaneous signal from $N = 102$ MEG sensors at time t_j. We analyze the multivariable MEG signal

$$\mathbf{X} = \{\mathbf{X}^j\}\big|_{j=1}^{1000} \tag{2}$$

for 1 s after the Necker cube demonstration, with time discretization step $\Delta t = 1$ ms as a discrete sequence of 1000 instantaneous brain state vectors [Eq. (1)].

The MLP scheme used throughout our work is shown in Fig. 2(b). One can see that the time series from the 102-dimensional input layer, according to the dimension of information vector $\mathbf{X}^j$, are fed into each computational unit or node (artificial neuron) of the first hidden layer with $h_1 = 15$ nodes. Then, the h_1-dimensional output vector from the first hidden layer is applied to the second hidden layer with $h_2 = 5$ computational units. Afterwards, the h_2-dimensional output vector from the second hidden layer is applied to the output layer, which produces a whole neural network reply Y^j to the input information vector $\mathbf{X}^j$. Since we need to classify only two brain states corresponding to the perception of either left- or right-oriented Necker cube (state "0" or state "1," respectively), the output layer of the MLP consists of only one computational unit, which calculates binary output value Y^j. So, feeding MLP with input discrete sequence [Eq. (2)], we get the MLP response in the form of discrete time series as

$$\mathbf{Y} = \{Y^j\}\big|_{j=1}^{1000}. \tag{3}$$

Each MLP layer processes the input vector according to the following equation:

$$\mathbf{u} = f(\mathbf{W}\mathbf{x} + \mathbf{b}), \tag{4}$$

where $\mathbf{u}$ is the output layer vector, $\mathbf{x}$ is the input layer vector, $\mathbf{W}$ is the weight matrix, $\mathbf{b}$ is the bias, and $f(x)$ is the logistic transfer function defined as

$$f(x) = \frac{1}{1 + e^{-x}}. \tag{5}$$

Taking into account the architecture of MLP, presented in Fig. 2, the final response of neural network Y^j to input vector $\mathbf{X}^j$ is calculated as follows:

$$Y^j = f\left(\mathbf{W}_{out} f\left(\mathbf{W}_{H_2} f\left(\mathbf{W}_{H_1}\mathbf{X}^j + \mathbf{b}_{H_1}\right) + \mathbf{b}_{H_2}\right) + \mathbf{b}_{out}\right).$$

We suppose that MLP outputs $Y^j < 0.5$ and $Y^j > 0.5$ detect instant perception of the presented Necker cube as left-oriented (brain state "0") and right-oriented (brain state "1"), respectively.

The optimization of the MLP parameters, namely, weight matrices $\mathbf{W}_{H_1}$, $\mathbf{W}_{H_2}$, $\mathbf{W}_{out}$ and biases $\mathbf{b}_{H_1}$, $\mathbf{b}_{H_2}$, $\mathbf{b}_{out}$ was provided during the learning process by minimizing the mean squared error (MSE):

$$\mathrm{MSE} = \sqrt{\frac{1}{K}\sum_{k=1}^{K}(d_k - Y_k)^2}, \tag{6}$$

where K is the number of samples in the training dataset, Y_k is the value of the MLP response to each k sample from the entire dataset, and d_k is the value of a desired MLP response which we wish the MLP learns during the process. It should be noted that the learning procedure was performed separately for each volunteer. We applied the Levenberg-Marquardt algorithm (LMA) to provide accurate training of the MLP.[34] The LMA was chosen to obtain better convergence of the MSE-function, however, it required significantly long computational time to precisely define the unknown parameters.

For the learning process, we prepared training datasets containing MEG trials and desired answers which we wanted the ANN to learn. It should be noted that in the second experimental session the participants did not press a key, and therefore, the information about the interpretation of the ambiguous images was unknown. Nevertheless, the results of the first experimental session have shown that all participants interpreted correctly the orientation of the evident Necker cube image with intensities $I=0.1$ and $I=0.9$. In other words, the presentation of the evident Necker cube image excited the well-defined brain states "0" and "1" corresponding to the left- and right-oriented cubes, respectively. Therefore, it was possible to align MEG trials after evident cube demonstrations with desired answers. Based on this observation, we composed training datasets for each participant from 20 MEG signals of 1-s duration (for total 20 000 samples taken with a 1-kHz sampling frequency) recorded from each subject after demonstration of clearly left- and right-oriented Necker cubes (see Subsec. II D). The validation dataset was composed of 10 remaining trials (10 000 samples).

The results of the training and validation processes are given in Fig. 3. We first checked MLP performance using only the set of 32 signals taken from MEG sensors, corresponding to the occipital lobe [Figs. 3(a) and 3(b)]. We found that classification accuracy in this case was sufficiently small (of the order of 63%). However, the account for the signals from all 102 MEG sensors [Figs. 3(c) and 3(d)] provided a significant increase in the MLP classification accuracy. One can see that the trained MLP handled accurate classification of instantaneous brain states corresponding to the left- and right-oriented cube interpretations (~86%). Based on this accuracy test, we conclude that the consideration of processes in the occipital lobe only, associated with low-level visual representation is not enough for precise detection of brain states related to the decision-making process. Actually, several studies of bistable images using event-related potentials, EEG trials, and fMRI showed that visual perception was accompanied by activation of specific brain areas and deactivation of others.[35–37] In particular, a chain of event-related potential components was found during observation of a Necker cube lattice which led to spontaneous perceptual reversals.[37] Our results show that significant changes in the event-related potentials observed in the occipital cortex provide accurate classification of brain states related to the decision-making process. One should also take into account the brain activity in different brain areas due to the fact that the decision-making is a complex higher-level process which includes the information transfer over the whole cortex network with activation of frontal, parietal, and occipital areas.

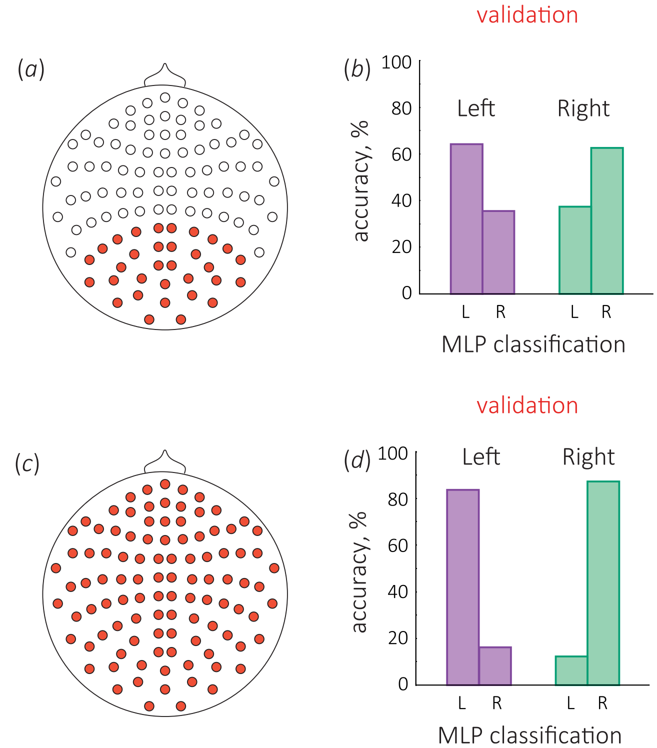

FIG. 3. Illustration of MLP validation accuracy and comparison of its value for different sets of MEG channels. Here and below, *purple* boxes and curves correspond to left-oriented Necker cube interpretation (brain state "0") and *green* boxes and curves to right-oriented cube (brain state "1"). Panel (b) shows the value of MLP accuracy calculated by taking into account only signals from 32 MEG sensors corresponding to occipital lobe [scheme (a)]. In contrast, panel (d) illustrates MLP accuracy while considering signals from all MEG sensors [scheme (c)].

G. ANN output analysis

In order to find trends and general features of the decision-making process and highlight the most significant brain areas, we carried out the MLP response analysis over experimental sessions individually for each participant.

Let $Y_n^I(t)$ be the MLP response to the MEG signals taken during the observation of the Necker cube image with edges intensity I during the n-th experimental session. Then,

$$\langle Y^I\rangle(t) = \frac{1}{N}\sum_{n=1}^{N} Y_n^I(t) \tag{7}$$

is the averaged MLP response to the MEG signals taken during the observation of a Necker cube image with edges intensity I over N experimental sessions, and

$$\sigma^I(t) = \sqrt{\frac{1}{N}\sum_{n=1}^{N}\left(Y_n^I(t) - \langle Y^I\rangle(t)\right)^2} \tag{8}$$

is the standard deviation of the MLP responses over N sessions. We suggest standard deviation σ to be a measure of decision-making uncertainty.

We suppose that the interpretation process of identical images should proceed in approximately the same way. Thus, the MEG traces corresponding to certain decisions about observed image interpretation should be characterized by a small variation of the MLP response over different trials. In contrast, a large variation of instantaneous MLP responses over different trials should be inherent to traces corresponding to high decision-making uncertainty. So, one can introduce the threshold value σ_{tr} above which one can judge that the brain is typically uncertain about the decision-making at time t_i of the considered 1-s interval.

To define the threshold σ_{tr} and distinguish between decision-making uncertainty and certain brain states, we calculate the MLP output standard deviation during observation of the ambiguous Necker cube with $I = 0.5$. The observation of this image cannot provide any certain decision on the cube orientation because all edges have the same contrast. Indeed, a typical MLP response trace, corresponding to the perception this image is characterized by multiple irregular switches between "0" and "1" [see Fig. 4(c)]. The standard deviation calculated using Eq. (8) and its distribution $\rho(\sigma)$ exhibit the values of $\sigma^{0.5} \geq 0.3$. Based on this result, we define the threshold value σ_{tr} as the 5% percentile of the $\sigma^{0.5}$ distribution.

Values of $\sigma^I(t)$ with $I \neq 0.5$ are compared with the threshold σ_{tr}. If $\sigma^I(t) < \sigma_{tr}$, we state that the participant is typically certain about the cube interpretation, whereas $\sigma^I(t) \geq \sigma_{tr}$ indicates a decision-making uncertainty state.

On the base of the above definition, we also introduce the uncertainty measure $U(I)$ characterized the individual level of decision-making uncertainty during the observation of the bistable image with parameter I, as follows:

$$U(I) = \frac{1}{T}\sum_{i=1}^{T}\Theta\left(\sigma^I(t_i) - \sigma_{tr}\right), \tag{9}$$

where T is a number of MEG trial samples and $\Theta(\bullet)$ is a Heaviside step-function. The uncertainty measure $U(I)$ is a portion of the 1-sec time interval during which the brain is uncertain in decision-making.

III. RESULTS AND DISCUSSION

The observation of ambiguous Necker cubes leads to switches of visual perception between two alternative states associated with left and right cube orientations. Each state is observed in the MEG data when the presented cubes are non-ambiguous, i.e., when $I = 0$ or $I = 1$. Thus, we consider the human brain processing ambiguous stimulus, as a bistable dynamical system,[23,24] whose state is described by the vector [Eq. (1)] to which the MLP with the input matrix [Eq. (2)] is applied.

At the first stage, the MLP neural network was trained and validated individually for each of five subjects participated in the MEG experiment. The mean accuracy in MLP classification obtained during the validation procedure for all subjects was close to 86%. The application of well trained MLP allowed us to assess important features of the human decision-making process.

The time series in Figs. 4(a)–4(c) show typical MLP responses to individual MEG trials when cubes with different

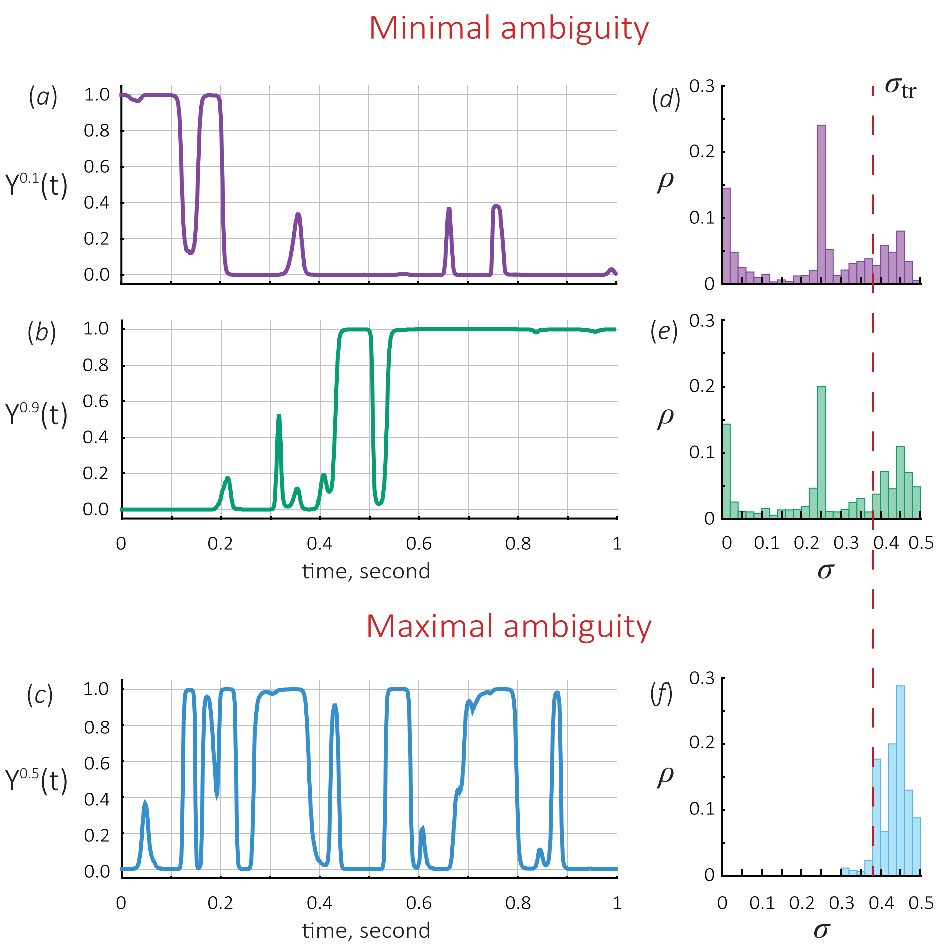

FIG. 4. (a)-(c) Individual MLP response traces Y(t) and (d-f) probability distribution of standard deviation $\rho(\sigma)$ calculated over MEG experimental sessions. Panels [(a) and (d)] and [(b) and (e)] show the MLP responses to the interpretation of low ambiguous left- and right-oriented Necker cubes with $I = 0.1$ and $I = 0.9$, respectively. Panels (c) and (f) illustrate the MLP response to the interpretation of a highly-ambiguous cube with $I = 0.5$. The dashed line denotes standard deviation threshold σ_{tr}.

ambiguity were presented. On can see in Figs. 4(a) and 4(b) that in the case of a low-ambiguous left- or right-oriented cube, the MPL response curve, after short transient fluctuations, converges to a stable state "0" or "1," respectively. We refer such a behavior of the ANN trace to as a decision-making certainty since ANN handles the identification of well-established and temporally stable brain states associated with left- or right-oriented cube interpretation. Instead, the observation of a highly-ambiguous image is characterized by multiple irregular switches between "0" and "1" values, as seen in Fig. 4(c). We interpret the latter as the ANN uncertainty which is a consequence of a doubt in decision-making. One of the measures characterizing the decision-making process in average over experimental sessions is standard deviation σ of the MLP output, presented in Figs. 4(d)–4(f). While in the former case the standard deviation is distributed in a wide range from 0 to 0.5, in the latter case the standard deviation is localized in a narrow range above the threshold σ_{tr} to 0.5 indicating decision-making uncertainty.

Figure 5 shows the sequence of averaged MLP outputs along with traces of standard deviation corresponding to MEG recordings taken during 1 s after demonstration of the Necker cube with different edges intensities I. The left and right columns represent the MLP outputs and standard deviations obtained from MEG signals corresponding to the left- and right-oriented cubes with the same value of relative edge intensity $\Delta I = |I - 0.5|$ or ambiguity degree. The ambiguity degree varied from 0 and 0.5 is used as a control parameter. The lower ΔI, the higher the ambiguity. A highly ambiguous cube with $I = 0.5$ has $\Delta I = 0$, while non-ambiguous cubes with $I = 0$ or $I = 1$ have $\Delta I = 0.5$. Figures 5(a) and 5(d) demonstrate that the subject clearly interpreted the orientation of the presented Necker cubes while observing images with evident orientations ($\Delta I = 0.4$); the MLP outputs converge to either 0 or 1 in the case of left- or right-oriented cubes, respectively.

We can see in Figs. 5(a) and 5(d) that the standard deviation is below the threshold ($\sigma < \sigma_{tr}$) during a major part of the 1-sec interval. Note, that the convergence of $\langle Y \rangle$ to 0 and 1 is accompanied by the drop of σ. The analysis of the MLP output curves together with the standard deviation allowed us to conclude that the subjects made a decision on the cube orientation after a short transient time τ when he/she was uncertain about the image interpretation. Thus, we can divide

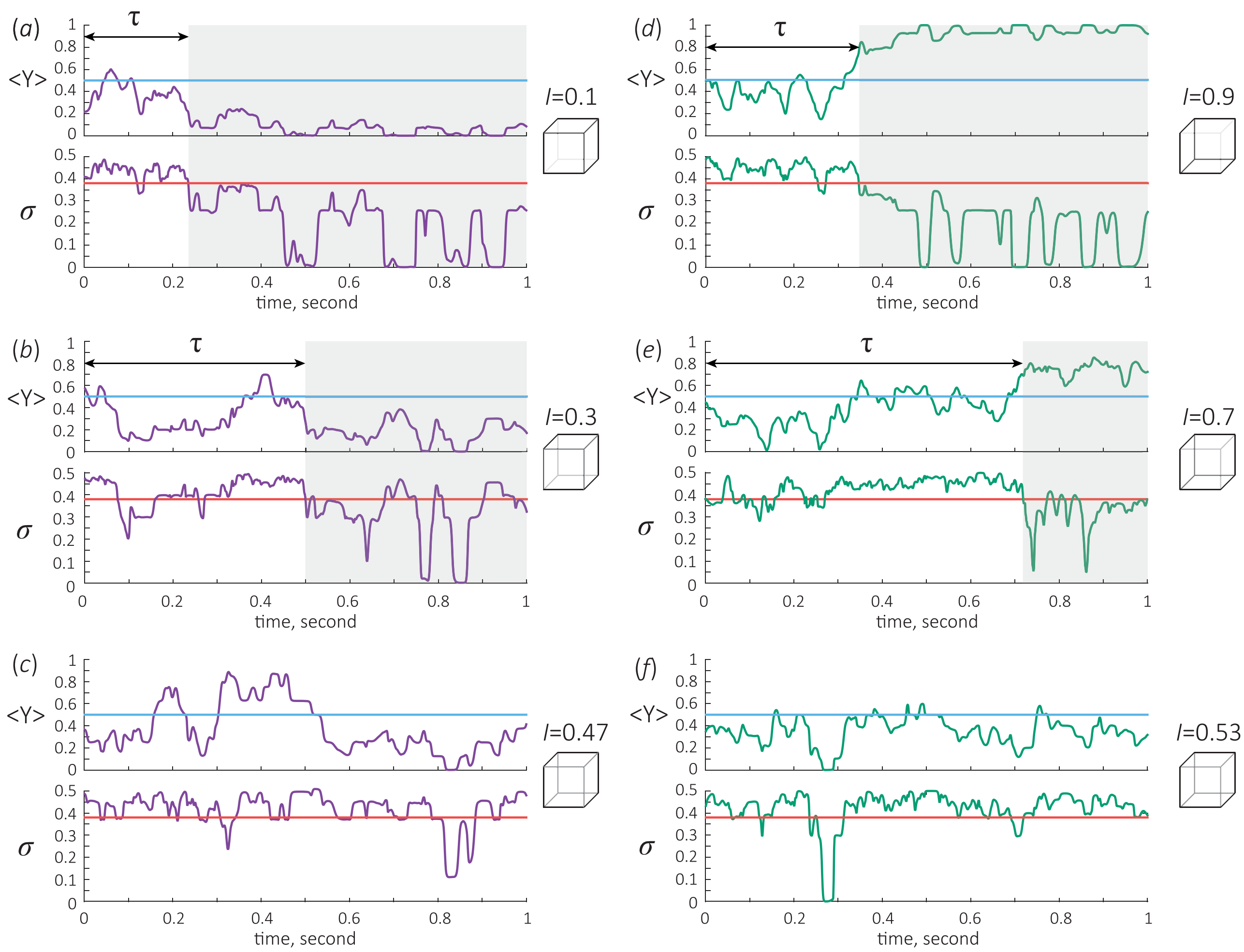

FIG. 5. Sequence of MLP responses averaged over experimental sessions $\langle Y \rangle$ (upper traces) and standard deviation σ (lower traces). Decision-making process in interpretation of (a) and (d) low-ambiguous, (b) and (e) medium-ambiguous, and (c) and (f) high-ambiguous images is shown. The corresponding Necker cube images with specified edges intensities I are shown in the right-hand side of each panel. Gray areas highlight the regions of 1 second trials, which are significant in terms of decision-making certainty.

the perception process into two stages: stage I (decision is in process, which can be considered as the time of decision-making uncertainty) and stage II (decision is already made, which can be considered as a stable well-recognized brain state). Therefore, the value of τ characterizes the time interval required for visual stimulus processing and decision-making on image interpretation.

Figures 5(b) and 5(e) show the curves of the averaged MLP output and standard deviation corresponding to the observation of images with medium degree of ambiguity. One can see that an increase in ambiguity leads to an increase in the duration τ of the transient stage I required for visual stimulus processing via higher-nervous activity, because high-ambiguous images are more complex for visual perception and further interpretation. The interpretation process of the Necker cube with small ΔI qualitatively differs from the interpretation of low-ambiguous images. Figures 5(c) and 5(f) illustrate the subject uncertainty on the cube orientation during the observation of high-ambiguous Necker cubes with $\Delta I = 0.03$. The features of the human brain behavior detected via MLP allows one to distinguish different stages of the decision-making process and decide whether a subject (in average) handles the interpretation successfully or not, as well as to estimate how difficult it was for him to interpret the observed image. Thus, looking at the averaged MLP output and standard deviation, one can realize whether, typically, the participant has already interpreted the observed Necker cube or still remains uncertain about its orientation.

Finally, Fig. 6 illustrates the values of uncertainty $U(I)$ calculated according to Eq. (9) and time lag τ in decision-making. The data were averaged over the group of participants. One can see from Fig. 6(a) that $U(I)$ grows up as ambiguity increases and has a well-pronounced peak at $I = 0.5$ (highest ambiguity). Figure 6(b) also shows the explicit tendency in increasing time τ needed for the brain to perceive and interpret the demonstrated image. It should be noted that both dependencies $U(I)$ and $\tau(I)$ are asymmetric with respect to $I = 0.5$ that indicates lower level in decision-making uncertainty while observing left-oriented Necker cube images. Such left-oriented perceptual bias observed in the data of all participants may be caused by different reasons, e.g., the influence of the leading eye,[38] features of visual information interpretation conditioned by left-to-right reading or left hemispherical attentional bias.[39,40]

The experimental data were analyzed using paired t-test. According to the obtained p-values, the significant changes in U and τ are marked by "*" for $p < 0.05$ and "**" for $p < 0.001$. It can be seen that both $U(I)$ and τ exhibit significant changes as the edges intensity varies, more pronounced for high and low I associated with unambiguous cases ($p < 0.001$). On the contrary, for $I \approx 0.5$, the changes are less significant ($p < 0.05$).

Thus, summarizing these results, we can say that a growth of uncertainty in decision-making was observed not only in one participant, but was peculiar to the whole group. The features of the decision-making process, detected via artificial intelligence tools, namely, the duration of image perception τ and uncertainty measure U helped us to distinguish between clear interpretation of the visual stimuli and the state

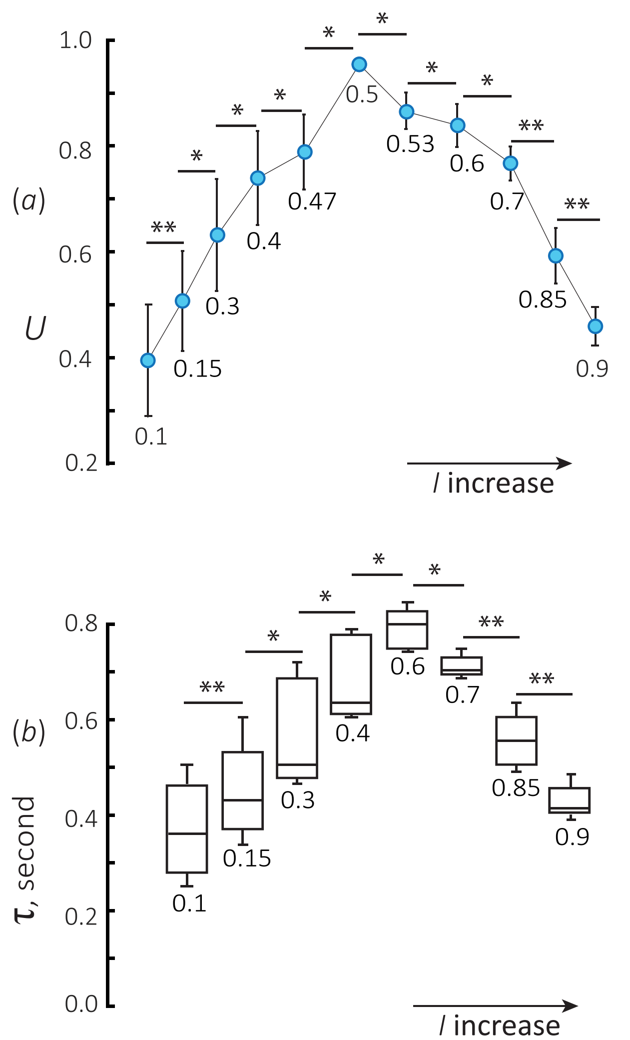

FIG. 6. Statistical characteristics of Necker cube interpretation for the group of subjects, calculated on the base of MLP processing of experimental MEG signals. (a) Uncertainty measure $U(I)$ averaged over the group of participants. Error-bars show the standard deviation. (b) Boxes and whiskers indicate time lags $\tau(I)$ for different edges intensities I. The stars "*" and "**" indicate statistical significance of $p < 0.05$ and $p < 0.001$, respectively. The p-values were calculated via paired t-test.

of uncertainty, without the analysis of direct answers from the subject, but solely from his/her brain activity. While studying mechanisms of perceptual decision-making, Heekeren *et al.*[41] noted that "*During a rainstorm, however, the sensory input is noisier, and thus you have to look longer to gather more sensory data to make a decision about the person at the light and the appropriate behavioural response*." Using our approach, we can estimate how long the decision-marking process will take place. Finally, it should be noted that the provided measures are able to indicate the difference in interpretation of left- and right-oriented Necker cube images, and that the latter induces higher level of decision-making uncertainty.[38–40]

IV. CONCLUSIONS

The artificial neural network approach was applied for recognition and classification of MEG trials associated with perception of ambiguous graphical objects. We trained ANN to recognize interpretations of fully left- or right-oriented Necker cubes. The comparison of averaged ANN outputs along with their standard deviation over multiple experimental sessions, obtained for these cubes over a 1-s interval allowed accessing some important features of ambiguous images interpretation from the decision-making viewpoint.

First, we have shown that interpretation of low- and medium-ambiguous images differed from interpretation of high-ambiguous images. The interpretation process of low- and medium-ambiguous images can be divided into two stages: in stage I the subject is uncertain about the decision, and in stage II the decision is made. The duration of stage I increases as the image ambiguity grows. During the observation of high-ambiguous images, the human brain is mostly in a decision-making uncertainty state characterized by multiple irregular switches between ANN output values "0" and "1."

Second, we have introduced quantitative measures U and τ for estimating the level of human decision-making uncertainty based on the analysis of neurophysiological signals of the brain activity without any visual or audio contact with the subject. Third, the analysis of uncertainty measure U over the group of participants allowed us to reveal a particular feature in the perception of ambiguous images: the perception of right-oriented Necker cubes resulted in a higher level of decision-making uncertainty as compared with left-oriented cubes.

The obtained results are very promising for application of artificial neural networks in intelligent systems with the aim of quantitative description of the decision-making process. Our results can also be useful for the development of new generations of brain-computer interfaces able to control and enhance the human ability to make a decision in stressful situations.[42–45]

ACKNOWLEDGMENTS

We would like to express our gratitude to the Reviewers for comments and suggestions that have improved the article. This work has been supported by Russian Science Foundation (Grant No. 17–72-30003) in the part of development of the method of decision-marking uncertainty recognition based on artificial neuronal network and processing experimental MEG data. A.N.P. acknowledges the support from the Ministry of Economy and Competitiveness (Spain) (Project No. SAF2016–80240) for performing MEG experiments.

[1]B. Müller, J. Reinhardt, and M. T. Strickland, *Neural Networks: An Introduction* (Springer Science & Business Media, 2012).
[2]J. Schmidhuber, "Deep learning in neural networks: An overview," Neural Networks **61**, 85–117 (2015).
[3]Y. LeCun, Y. Bengio, and G. Hinton, "Deep learning," Nature **521**, 436–444 (2015).
[4]M. Lukoševičius and H. Jaeger, "Reservoir computing approaches to recurrent neural network training," Comput. Sci. Rev. **3**, 127–149 (2009).
[5]M. Lee, S. Bressler, and R. Kozma, "Advances in cognitive engineering using neural networks," Neural Networks **92**, 1–2 (2017).
[6]L. Guo, D. Rivero, and A. Pazos, "Epileptic seizure detection using multiwavelet transform based approximate entropy and artificial neural networks," J. Neurosci. Methods **193**, 156–163 (2010).
[7]S. C. Jun and B. A. Pearlmutter, "Fast robust subject-independent magnetoencephalographic source localization using an artificial neural network," Hum. Brain Mapping **24**, 21–34 (2005).
[8]M. Misaki and S. Miyauchi, "Application of artificial neural network to FMRI regression analysis," Neuroimage **29**, 396–408 (2006).
[9]T. Emoto, U. R. Abeyratne, Y. Chen, I. Kawata, M. Akutagawa, and Y. Kinouchi, "Artificial neural networks for breathing and snoring episode detection in sleep sounds," Physiol. Meas. **33**, 1675 (2012).
[10]L. Quitadamo, F. Cavrini, L. Sbernini, F. Riillo, L. Bianchi, S. Seri, and G. Saggio, "Support vector machines to detect physiological patterns for EEG and EMG-based human–computer interaction: A review," J. Neural Eng. **14**, 011001 (2017).
[11]A. E. Hramov, S. V. Pchelintseva, A. E. Runnova, V. Y. Musatov, V. V. Grubov, M. O. Zhuravlev, V. A. Maksimenko, A. A. Koronovskii, and A. N. Pisarchik, "Classifying the perceptual interpretations of a bistable image using EEG and artificial neural networks," Front. Neurosci. **11**, 674 (2017).
[12]E. S. Nurse, P. J. Karoly, D. B. Grayden, and D. R. Freestone, "A generalizable brain-computer interface (BCI) using machine learning for feature discovery," PloS one **10**, e0131328 (2015).
[13]G. Ghazaei, A. Alameer, P. Degenaar, G. Morgan, and K. Nazarpour, "Deep learning-based artificial vision for grasp classification in myoelectric hands," J. Neural Eng. **14**, 036025 (2017).
[14]Y. Ma, X. Ding, Q. She, Z. Luo, T. Potter, and Y. Zhang, "Classification of motor imagery EEG signals with support vector machines and particle swarm optimization," Comput. Math. Methods Med. **2016**, 4941235.
[15]M. H. Alomari, A. Samaha, and K. AlKamha, "Automated classification of L/R hand movement EEG signals using advanced feature extraction and machine learning," International Journal of Advanced Computer Science and Applications **4**(6) (2013).
[16]W. Webber, R. P. Lesser, R. T. Richardson, and K. Wilson, "An approach to seizure detection using an artificial neural network (ANN)," Electroencephalogr. Clin. Neurophysiol. **98**, 250–272 (1996).
[17]P. Fergus, D. Hignett, A. Hussain, D. Al-Jumeily, and K. Abdel-Aziz, "Automatic epileptic seizure detection using scalp EEG and advanced artificial intelligence techniques," BioMed Res. Int. **2015**, 986736.
[18]C. Galletly, C. Clark, and A. McFarlane, "Artificial neural networks and psychiatric disorders," Brit. J. Psychiatry **169**, 793–794 (1996).
[19]E. Grossi, F. Veggo, A. Narzisi, A. Compare, and F. Muratori, "Pregnancy risk factors in autism: A pilot study with artificial neural networks," Pediatr. Res. **79**, 339–347 (2015).
[20]Z. Zhang, F. Vanderhaegen, and P. Millot, "Prediction of human behaviour using artificial neural networks," Lecture Notes Comput. Sci. **3930**, 770 (2006).
[21]L. Necker, "Observations on some remarkable phenomena seen in Switzerland and on an optical phenomenon which occurs on viewing of a crystal or geometrical solid," Philos. Mag. **111**, 329–337 (1832).
[22]B. Mathes, D. Strüber, M. A. Stadler, and C. Basar-Eroglu, "Voluntary control of Necker cube reversals modulates the EEG delta-and gamma-band response," Neurosci. Lett. **402**, 145–149 (2006).
[23]A. N. Pisarchik, R. Jaimes-Reategui, C. D. A. Magallón-Garcia, and C. O. Castillo-Morales, "Critical slowing down and noise-induced intermittency in bistable perception: Bifurcation analysis," Biol. Cybern. **108**, 397–404 (2014).
[24]A. E. Runnova, A. E. Hramov, V. Grubov, A. A. Koronovsky, M. K. Kurovskaya, and A. N. Pisarchik, "Theoretical background and experimental measurements of human brain noise intensity in perception of ambiguous images," Chaos, Solitons Fractals **93**, 201–206 (2016).
[25]A. E. Hramov, M. K. Kurovskaya, A. E. Runnova, M. O. Zhuravlev, V. V. Grubov, A. A. Koronovskii, A. N. Pavlov, and A. N. Pisarchik, "Intermittent behavior in the brain neuronal network in the perception of ambiguous images," in *Dynamics and Fluctuations in Biomedical Photonics XIV* (International Society for Optics and Photonics, 2017), p. 1006314.
[26]A. N. Pisarchik, I. A. Bashkirtseva, and L. Ryashko, "Controlling bistability in a stochastic perception model," Eur. Phys. J. Spec. Top. **224**, 1477–1484 (2015).
[27]I. A. Bashkirtseva and L. Ryashko, "Stochastic sensitivity of a bistable energy model for visual perception," Indian J. Phys. **91**, 57–62 (2017).
[28]A. Pastukhov, P. E. Garcia-Rodriguez, J. Haenicke, A. Guillamon, G. Deco, and J. Braun, "Multi-stable perception balances stability and sensitivity," Front. Comput. Neurosci. **7**, 17 (2013).
[29]R. H. S. Carpenter, "Analysing the detail of saccadic reaction time distributions," Biocybern. Biomed. Eng. **32**, 49–63 (2012).
[30]I. Merk and J. Schnakenberg, "A stochastic model of multistable visual perception," Biol. Cybern. **86**, 111–116 (2002).
[31]D. A. Leopold, M. Wilke, A. Maier, and N. K. Logothetis, "Stable perception of visually ambiguous patterns," Nature Neurosci. **5**, 605–609 (2002).

[32]S. Taulu and R. Hari, "Removal of magnetoencephalographic artifacts with temporal signal-space separation: Demonstration with single-trial auditory-evoked responses," Hum. Brain Mapping **30**, 1524–1534 (2009).
[33]F. Amato, A. López, E. M. Peña-Méndez, P. Vaňhara, A. Hampl, and J. Havel, "Artificial neural networks in medical diagnosis," J. Appl. Biomed. **11**, 47–58 (2013).
[34]T. Strutz, *Data Fitting and Uncertainty (a Practical Introduction to Weighted Least Squares and Beyond)*, 2nd ed. (Springer, 2016).
[35]T. Inui, S. Tanaka, T. Okada, S. Nishizawa, M. Katayama, and J. Konishi, "Neural substrates for depth perception of the Necker cube: A functional magnetic resonance imaging study in human subjects," Neurosci. Lett. **282**, 145–148 (2000).
[36]T. J. Müller, A. Federspiel, H. Horn, K. Lovblad, C. Lehmann, T. Dierks, and W. Strick, "The neurophysiological time pattern of illusionary visual perceptual transitions: A simultaneous EEG and fMRI study," Int. J. Psychophysiol. **55**, 299–312 (2005).
[37]J. Kornmeier and M. Bach, "Bistable perception along the processing chain from ambiguous visual input to a stable percept," Int. J. Psychophysiol. **62**, 345–349 (2006).
[38]A. P. Mapp, H. Ono, and R. Barbeito, "What does the dominant eye dominate? a brief and somewhat contentious review," Atten. Percept. Psychophys. **65**, 310–317 (2003).
[39]S. Chokron and M. De Agostini, "Reading habits and line bisection: A developmental approach," Cognitive Brain Res. **3**, 51–58 (1995).
[40]M. E. Nicholls and G. R. Roberts, "Can free-viewing perceptual asymmetries be explained by scanning, pre-motor or attentional biases?," Cortex **38**, 113–136 (2002).
[41]H. R. Heekeren, S. Marrett, P. A. Bandettini, and L. G. Ungerleider, "A general mechanism for perceptual decision-making in the human brain," Nature **431**, 859–862 (2004).
[42]K. Starcke and M. Brand, "Decision making under stress: A selective review," Neurosci. Biobehav. Rev. **36**, 1228–1248 (2012).
[43]S. E. Wemm and E. Wulfert, "Effects of acute stress on decision making," Appl. Psychophysiol. Biofeedback **42**, 1–12 (2017).
[44]S. Amitay, J. Guiraud, E. Sohoglu, O. Zobay, B. A. Edmonds, Y.-X. Zhang, and D. R. Moore, "Human decision making based on variations in internal noise: An EEG study," PloS one **8**, e68928 (2013).
[45]R. Poli, D. Valeriani, and C. Cinel, "Collaborative brain-computer interface for aiding decision-making," PloS one **9**, e102693 (2014).